

Analysis of Cracked Body Strengthened by Adhesively Bonded Patches by BEM-FEM Coupling

*Binh Viet Pham¹, Thai Binh Nguyen², and †Jaron Rungamornrat³

¹Applied Mechanics and Structures Research Unit, Department of Civil Engineering, Faculty of Engineering, Chulalongkorn University, Bangkok 10330, Thailand.

²Faculty of Civil Engineering, Ho Chi Minh City University of Technology, Vietnam National University Ho Chi Minh City, 740128, Vietnam

³Applied Mechanics and Structures Research Unit, Department of Civil Engineering, Faculty of Engineering, Chulalongkorn University, Bangkok 10330, Thailand.

*Presenting author: phamvietbinh872426@gmail.com

†Corresponding author: jaron.r@chula.ac.th

Abstract

This paper presents an efficient numerical technique capable of handling the stress analysis of three-dimensional cracked bodies strengthened by adhesively bonded patches. The proposed technique is implemented within the framework of the coupling of the weakly singular boundary integral equation method and the standard finite element procedure. The former is applied to efficiently treat the elastic body containing cracks whereas the latter is adopted to handle both the adhesive layers and patches. The approximation of the near-front relative crack-face displacement is enhanced by using local interpolation functions that can capture the right asymptotic behaviour. This also offers the direct calculation of the stress intensity factors along the crack front. A selected set of results is reported to demonstrate the capability of the proposed technique and the influence of various parameters on the performance of the strengthening.

Keywords: Boundary integral equation method, Bonded patches, Cracked body, Finite element method, Stress intensity factors

Introduction

Sustainability and integrity of engineering structures are ones among various crucial issues that must be properly integrated in the design procedure and the subsequent maintenance stage. It has been known that the presence of cracks/flaws/damages is one of the major causes of subsequent failures of components, parts of or the entire structures leading finally to the loss of their functions. For such reason, the strengthening of damaged/cracked structures at the earliest time as soon as they are detected during inspections is considered essential. Furthermore, the control of cracked structures after being strengthened is also one of vital tasks to evaluate the selected strengthening method so that those strengthened structures can maintain their bearing capacity.

Replacement of cracked or damaged parts can be time-consuming and expensive, and, in addition, requires a high level of expertise. It is usually more cost effective to strengthen those damaged components by using patching techniques. One of those methods, with adhesively bonded repairs, has been widely employed in practices. Many theoretical and empirical investigations have demonstrated the advantages of this particular method relative to other existing techniques for strengthening cracked structures due mainly to its cost effectiveness (e.g., [1-6]). In addition to their high stiffness and strength, the patches are structurally efficient and induce much less damages to the strengthened structures.

In the modeling point of view via a theory of linear elasticity and linear elastic fracture mechanics, the stress intensity factors along the crack front can be significantly reduced after

the cracked body is strengthened by attaching a patch over the cracked region (e.g., [6-19]). This is due to the fact that some of externally applied loads exerted to the cracked bodies are either shared by or transferred directly to the patches via the adhesive shear layers rendering the enhancement of stiffness near the patching region and the reduction of relative crack-face displacements. As a direct consequence, the growth of the cracks can be delayed or even ceased if the strengthening is properly designed. Evidences from past studies have indicated that various parameters including the dimensions and material properties of the strengthened structure, the patches, and the adhesive layers significantly affects the efficiency and effectiveness of the strengthening (e.g., [6-19]). The full investigation to understand the role of those parameters is considered essential and can assist designers/engineers in the optimization of their designs. While experimental studies offer an excellent means to establish a set of results reflecting real responses, the methods themselves consume a significant amount of resources and are quite limited to test settings. In particular, to assess efficiency and influence of the patches in the experiments, a large set of testing specimens including unpatched and patched cracked structures for various specimen configurations must be considered. An alternative approach is to adopt computer-based simulations via reliable mathematical models to perform such extensive parametric study. It is remarked, however, that to accomplish such an important task within a broad and general framework (e.g., three-dimensional settings, large-scale and complex cases), powerful and computationally efficient tools are prerequisite.

On the basis of an extensive literature survey, most of existing studies toward the development of computational techniques to assist the analysis and simulations of cracked components repaired by adhesively bonded patches were focused extensively on the two-dimensional framework and quite specific to certain settings such as the repair configurations and types of repaired structures. The enhancement of existing modeling tools to be capable of handling more complex and general scenarios such as fully three-dimensional and large scale problems is challenging and requires further extensive investigations.

Problem Formulation

Consider a three-dimensional, finite body containing both embedded and surface-breaking cracks and strengthened or reinforced by adhesively bonded patches as shown schematically in Figure 1. The cracked body is made of a homogeneous, generally anisotropic, linearly elastic material. The ordinary boundary of the cracked body, denoted by S_0 , consists of a surface S_u on which the displacement \mathbf{u}^{bu} is prescribed, a surface S_t on which the traction \mathbf{t}^{bt} is known a priori, and a flat or planar surface S_a on which the patch is attached. The surface of displacement discontinuity used to describe the crack in the undeformed state (i.e., stress-free state) is represented by a pair of geometrically identical surfaces, denoted by S_c^+ and S_c^- , and, in the present study, the attention is restricted only to the case that the crack surface is subjected to the point-wise self-equilibrated tractions; i.e., the prescribed tractions $\mathbf{t}^{b+}, \mathbf{t}^{b-}$ acting respectively to the surfaces S_c^+, S_c^- satisfy the condition $\mathbf{t}^{b+} + \mathbf{t}^{b-} = \mathbf{0}$. Each patch is made of a homogeneous, linear elastic material and fully adhered to the cracked body on the surface S_a by means of an adhesive bonding material. The prescribed traction exerted to the surface of the patch, opposite to the attached surface, is denoted by \mathbf{t}^{p0} . In the present study, the thickness of the patches and adhesive layers is assumed relatively small in comparison with the characteristic dimension of the repaired body; as a result, the bending stiffness of the patches can be considered negligible whereas only the shear resistance is treated for the adhesive layers.

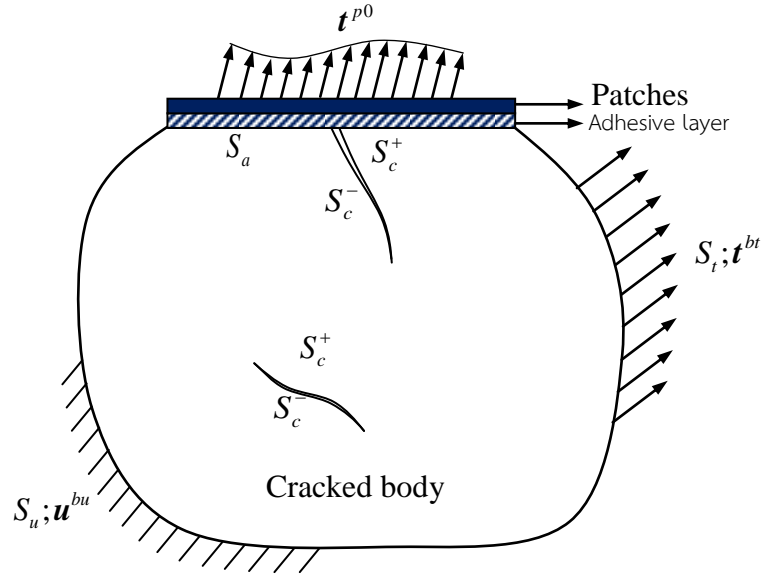


Figure 1. Schematic of a body containing embedded and surface-breaking cracks and strengthened by adhesively bonded patches

Since the thickness of each patch is sufficiently small and the bending effect can be ignored, its responses can then be properly modeled by a two-dimensional, plane-stress, linear elasticity theory. The final governing equation formulated in a local, two-dimensional, Cartesian coordinate system containing the patch by taking the in-plane displacement vector $\bar{\mathbf{u}}^{*p}$ as the primary unknown is given by

$$h_p \mathbf{L}^T \mathbf{C}^{*p} \mathbf{L} \bar{\mathbf{u}}^{*p} + \bar{\mathbf{s}}^{*pa} + \bar{\mathbf{s}}^{*p0} = \mathbf{0} \quad (1)$$

where \mathbf{L} is a conventional, two-dimensional differential operator transforming $\bar{\mathbf{u}}^{*p}$ into a vector containing independent in-plane strain components; the superscript “ T ” denotes the matrix transpose; h_p is the thickness of the patch; $\bar{\mathbf{s}}^{*p0}$ is a vector containing local components of the prescribed shear traction s^{p0} (i.e., the tangential component vector of the prescribed traction \mathbf{t}^{p0} on the plane of the patch), $\bar{\mathbf{s}}^{*pa}$ is a vector containing local components of the unknown shear traction exerted by the adhesive layer, and \mathbf{C}^{*p} is the elastic in-plane modulus matrix for the plane-stress case. An alternative weak-form of (1) can be readily established via a standard weighted residual technique and used as the basis in the discretization procedure.

From the assumption that the adhesive layer can transfer only shear across its thickness, the state of strain for the entire layer can be completely described by the out-of-plane shear strain. Since the thickness of the adhesive layer is infinitesimal in comparison with its planar dimensions, it is legitimate to assume that the out-of-plane shear strain components are uniform across the thickness or, equivalently, the in-plane displacement varies linearly across the thickness. The out-of-plane shear stress induced within the layer $\bar{\boldsymbol{\sigma}}^{*a}$ is then governed by

$$\bar{\boldsymbol{\sigma}}^{*a} = \frac{G_a}{h_a} (\bar{\mathbf{u}}^{*ap} - \bar{\mathbf{u}}^{*ab}) \quad (2)$$

where h_a is the thickness of the adhesive layer, G_a denotes the elastic shear modulus of the adhesive material, and $\bar{\mathbf{u}}^{*ap}$ and $\bar{\mathbf{u}}^{*ab}$ are values of the in-plane displacement at its interfaces connecting to the patch and the cracked body, respectively. Similarly, the weak-form statement of (2) can also be formulated by the weighted residual technique.

For the cracked body, the theory of linear elasticity with the absence of the body force is adopted and the key governing equations are formulated within the framework of boundary integral equations. In particular, the following pair of weakly singular, weak-form boundary integral equations for the displacements and tractions, proposed by Rungamornrat and Mear (2008a), is utilized to form a system of integral equations governing the unknown data on the boundary and crack surface:

$$\begin{aligned} \frac{1}{2} \int_{S_0} \tilde{\tau}_p(\mathbf{y}) u_p^b(\mathbf{y}) dS(\mathbf{y}) &= \int_{S_0} \tilde{\tau}_p(\mathbf{y}) \int_{S_0} U_j^p(\boldsymbol{\xi} - \mathbf{y}) t_j^b(\boldsymbol{\xi}) dS(\boldsymbol{\xi}) dS(\mathbf{y}) \\ &+ \int_{S_0} \tilde{\tau}_p(\mathbf{y}) \int_S G_{mj}^p(\boldsymbol{\xi} - \mathbf{y}) D_m v_j^b(\boldsymbol{\xi}) dS(\boldsymbol{\xi}) dS(\mathbf{y}) \\ &- \int_{S_0} \tilde{\tau}_p(\mathbf{y}) \int_S n_i(\boldsymbol{\xi}) H_{ij}^p(\boldsymbol{\xi} - \mathbf{y}) v_j^b(\boldsymbol{\xi}) dS(\boldsymbol{\xi}) dS(\mathbf{y}) \end{aligned} \quad (3)$$

$$\begin{aligned} -\frac{1}{2} \int_S \tilde{u}_k(\mathbf{y}) \tau_k^b(\mathbf{y}) dS(\mathbf{y}) &= \int_S D_t \tilde{u}_k(\mathbf{y}) \int_S C_{mj}^{tk}(\boldsymbol{\xi} - \mathbf{y}) D_m v_j^b(\boldsymbol{\xi}) dS(\boldsymbol{\xi}) dS(\mathbf{y}) \\ &+ \int_S D_t \tilde{u}_k(\mathbf{y}) \int_{S_0} G_{tk}^j(\boldsymbol{\xi} - \mathbf{y}) t_j^b(\boldsymbol{\xi}) dS(\boldsymbol{\xi}) dS(\mathbf{y}) \\ &+ \int_S \tilde{u}_k(\mathbf{y}) \int_{S_0} n_l(\mathbf{y}) H_{lk}^j(\boldsymbol{\xi} - \mathbf{y}) t_j^b(\boldsymbol{\xi}) dS(\boldsymbol{\xi}) dS(\mathbf{y}) \end{aligned} \quad (4)$$

where $S \equiv S_0 \cup S_c^+$ denotes the total boundary of the cracked body; $\tilde{\tau}_p$ is any sufficiently smooth test function defined on the ordinary boundary S_0 ; \tilde{u}_k is any sufficiently smooth test function defined on the total boundary S ; u_p^b and t_j^b are components of the displacement and traction on the ordinary boundary S_0 of the cracked body; n_i are components of the outward unit normal vector to the total boundary S ; $D_m = n_i \varepsilon_{ism} \partial / \partial \xi_s$ or $D_m = n_i \varepsilon_{ism} \partial / \partial y_s$ denotes the surface differential operator; U_j^p , C_{mj}^{tk} , G_{mj}^p , and H_{ij}^p are known fundamental solutions (see details of development and explicit expressions in Rungamornrat and Mear (2008a)); and v_j^b and τ_k^b are data defined by

$$v_j^b(\boldsymbol{\xi}) = \begin{cases} u_j^b(\boldsymbol{\xi}), & \boldsymbol{\xi} \in S_0 \\ \Delta u_j^b(\boldsymbol{\xi}), & \boldsymbol{\xi} \in S_c^+ \end{cases} \quad (5)$$

$$\tau_k^b(\boldsymbol{\xi}) = \begin{cases} t_k^b(\boldsymbol{\xi}), & \boldsymbol{\xi} \in S_0 \\ \Delta t_k^b(\boldsymbol{\xi}), & \boldsymbol{\xi} \in S_c^+ \end{cases} \quad (6)$$

in which $\Delta u_j^b = u_j^+ - u_j^-$ denotes the relative crack-face displacement and $\Delta t_k^b(\boldsymbol{\xi}) = t_k^{0+} - t_k^{0-}$ denotes the jump in the crack-face traction. In particular, for the self-equilibrated crack-face tractions, it yields $\Delta t_k^b(\boldsymbol{\xi}) = 2t_k^{0+}$. To form a system of integral equations governing all

unknown data on the boundary and the crack surface, the displacement boundary integral equation (3) is applied to the surface S_u with $\tilde{\tau}_p \equiv 0$ on $S_t \cup S_a$ whereas the traction boundary integral equation (4) is adopted for the remaining surface $S_t \cup S_a \cup S_c^+$ with $\tilde{u}_k \equiv 0$ on S_u .

A system of governing equations for the whole repaired cracked body shown in Figure 1 can now be obtained by combining the weak-form equations governing all patches, the weak-form equations governing all adhesive layers, and those governing the cracked body together with the continuity of the displacement and the traction along all material interfaces. The final system contains the following unknown functions: the shear stress within the adhesive layers $\bar{\sigma}^{*a}$, the in-plane displacement of the patch \bar{u}^{*p} , the displacement \mathbf{u}^{ba} on the surface S_a , the displacement \mathbf{u}^{bt} on the surface S_t , the traction \mathbf{t}^{bu} on the surface S_u , and the relative crack-face displacement $\Delta \mathbf{u}^b$.

Numerical Implementations

To discretize the governing weak-form equations for the patches and the adhesive layers, a standard finite element procedure for two-dimensional problems (e.g., [21-23]) is adopted. The unknown shear stress within the adhesive layer $\bar{\sigma}^{*a}$, the unknown in-plane displacement of the patch \bar{u}^{*p} , the unknown displacement on the surface of the cracked body \mathbf{u}^{ba} and all involved test functions are approximated using standard basis functions constructed locally on a finite element mesh consisting of standard, isoparametric, C^0 -elements.

To discretize the weakly-singular, weak-form integral equations governing the cracked body, Galerkin-based procedure similar to that proposed by Rungamornrat and Mear (2008b) is implemented. Due to the weakly singular feature of all involved integrals, both the trial and test functions can be approximated by a set of continuous basis functions constructed locally on a finite element mesh. In particular, standard isoparametric C^0 elements are employed everywhere in the solution discretization except in a local region of the crack surface adjacent to the crack front where special crack-tip elements, originally proposed by Li *et al.* (1998) and used later by Rungamornrat and Mear (2008b) to treat cracks in anisotropic media, are adopted. Element shape functions of such special crack-tip elements were properly enriched to contain the square-root-type behavior and accurately capture the near-front relative crack-face displacement (also see details in Yates *et al.* (2010) and Rungamornrat *et al.* (2019) for the structure of the near-front elastic field). Special quadrature rules proposed by Xiao (1998) are implemented to handle both weakly singular and nearly singular integrals and the efficient interpolation-based algorithm similar to that employed by Rungamornrat and Mear (2008b) is adopted to calculate all involved fundamental solutions for generally anisotropic materials.

The final system of linear algebraic equations resulting from the discretization of the governing equations of the patches, the adhesive layers, and the cracked body is solved by a selected efficient linear solver. The stress intensity factors along the crack front are then extracted directly from the solved relative crack-face displacement data together with the properties of the special crack-tip elements via the post-process formula proposed by Rungamornrat and Mear (2008b).

Numerical Results

To verify the implemented technique and also provide a set of results from a preliminary parametric study on the strengthening of cracked bodies, the following representative problem is chosen in numerical simulations. Consider a cube of an isotropic linearly elastic material that occupies the region $[-w, w] \times [-w, w] \times [-w, w]$ in space and contains a penny-shaped

crack of radius a as shown schematically in Figure 2. The crack lies on a plane $x_3 = 0$ with its center located at point $(0.4w, 0, 0)$. The crack front can be parametrized in terms of the angular position $\theta \in [0, 2\pi]$ by

$$x_1 = 0.4w - a \cos \theta, \quad x_2 = a \sin \theta, \quad x_3 = 0 \quad (7)$$

The cube is loaded by a uniform normal traction $t_3 = \sigma_0$ on the face $x_3 = w$ and the uniform normal traction $t_3 = -\sigma_0$ on the face $x_3 = -w$. To strengthen the cracked body, a patch of uniform thickness h_p is bonded to its entire face $x_1 = w$ by the adhesive layer of uniform thickness h_a . In the numerical study, the aspect ratio $a/w = 0.5$ and Young's modulus and Poisson's ratio given in Table 1 are considered and three meshes shown in Figure 3 are adopted.

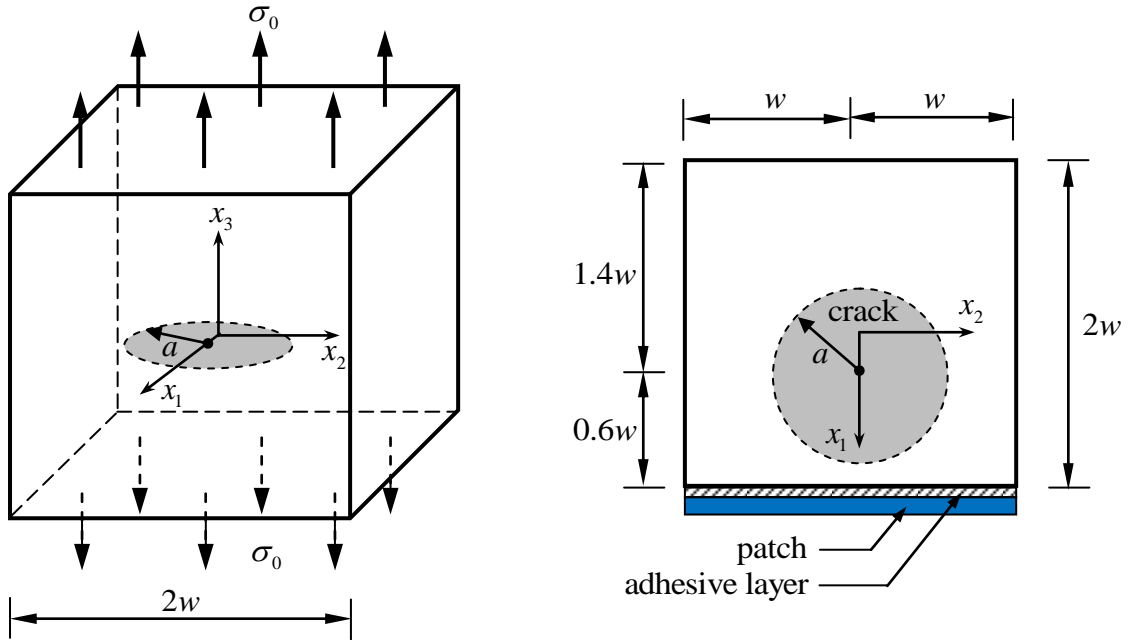


Figure 2. Schematic of cube material containing near-surface penny-shaped crack and strengthening by adhesively bonded patch

Table 1. Young's modulus and Poisson's ratio for cracked body, patch, and adhesive layer used in parametric study

Materials	Young's modulus ($\times 10^6$ psi)	Poisson's ratio
Cracked body	2.0	0.25
Patch	17.4	0.25
Adhesive layer	0.1	0.33

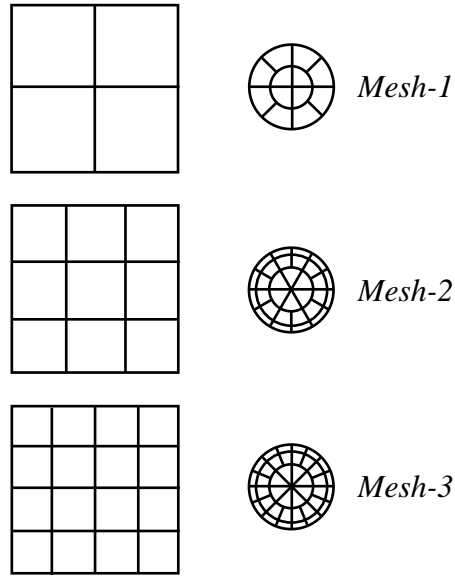


Figure 3. Three meshes adopted in analysis (only mesh of each face of cube is shown and it is identical to those for patch and adhesive layer)

Due to the symmetry and the loading condition considered, only the mode-I stress intensity factor (K_I) is non-zero. The normalized K_I obtained from the three meshes are reported in Figure 4 along with those generated by ABAQUS for the cases with and without the strengthening. It can be concluded from this set of results that numerical solutions converge as the mesh is refined and the good agreement between the converged and reference solution (with the difference within a fraction of one percent) is observed. Note in particular that relatively coarse meshes such as the Mesh-1 and Mesh-2 can also yield quite accurate results; this is due mainly to the use of special crack-tip elements in the approximation of the near-front relative crack-face displacement. After the cracked body is strengthened by the adhesively bonded patch, the stress intensity factor is significantly reduced especially in the region near the bonded patch.

After fully tested, the proposed technique can be further applied to study the influence of various strengthening parameters (e.g., thickness of the adhesive layer and thickness of the patch) on the strengthening performance. For instance, to explore the influence of the patch thickness on the reduction of the stress intensity factor of the crack in the representative problem, simulations can be carried out for different values of h_p while all other parameters remain fixed. A plot of the normalized mode-I stress intensity factor resulting from such simulations are reported in Figure 5, as examples, for $h_p/w = 0.00, 0.01, 0.02, 0.03, 0.04$. Besides the expected reduction of the stress intensity factor as the patch thickness increases (due to the increase in the stiffness after the strengthening), this piece of information is potentially useful in the selection of the patch thickness to confine the stress intensity factor below the tolerance or to prevent the subsequent crack growth. Similarly, the influence of the thickness of the adhesive layer on the response after the strengthening can also be investigated by carrying out simulations for various values of h_a while maintaining all other parameters. Results shown in Figure 6 are for the representative cracked body with three different values of the thickness of the adhesive layer (i.e., $h_a/w = 0.001, 0.005, 0.01$). It is evident that as the thickness of the adhesive layer increases, the apparent stiffness of the cracked body after strengthening tends to decrease.

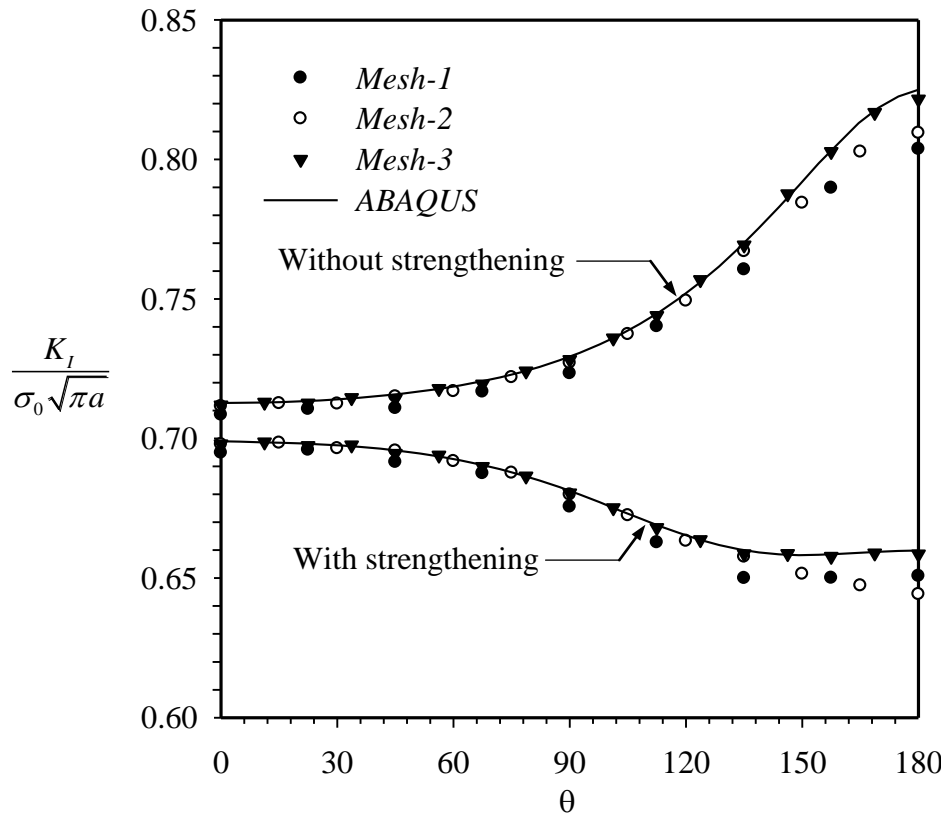


Figure 4. Normalized mode-I stress intensity factors of near-surface penny-shaped crack in cube of material under uniform normal traction σ_0 on its upper and lower faces. Results for the case of strengthening are reported for $h_a/w=0.001$ and $h_p/w=0.01$.

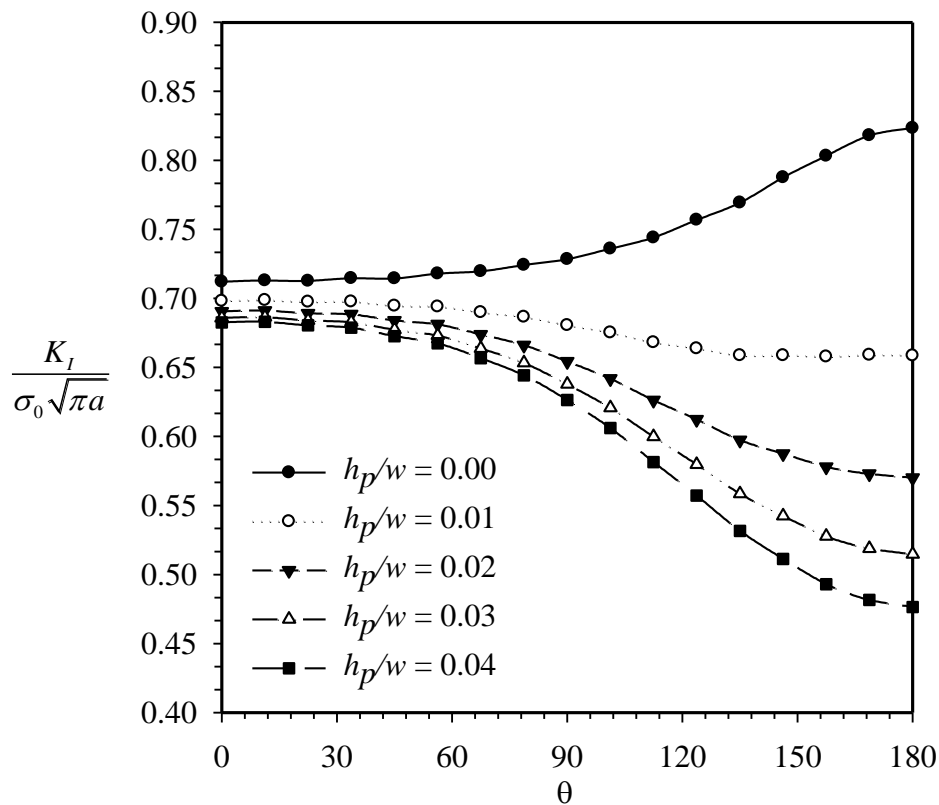


Figure 5. Influence of thickness of patch on normalized mode-I stress intensity factors for near-surface penny-shaped crack in cube of material

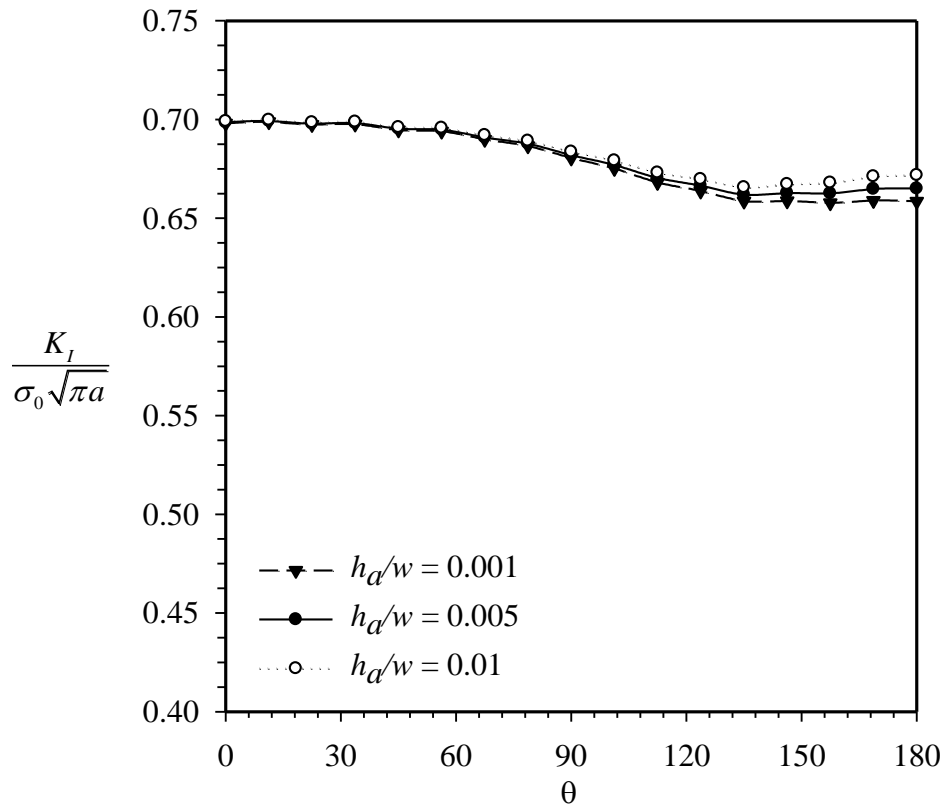


Figure 6. Influence of thickness of adhesive layer on normalized mode-I stress intensity factors for near-surface penny-shaped crack in cube of material

Conclusion and Remarks

The efficient and accurate BIE-FE coupling technique has been successfully implemented for the analysis of three-dimensional cracked bodies strengthened by adhesively bonded patch. The boundary integral equation method has been adopted to efficiently treat the cracked body whereas the standard finite element method has been utilized to handle both the adhesive layer and the patch. The near-front approximation of the relative crack-face displacement has been enhanced by means of using special crack-tip elements and this allows relatively coarse meshes to be employed in the discretization while still yielding sufficiently accurate fracture data along the crack front. Results from a numerical study have indicated that numerical solutions obtained from the proposed technique possess the good convergence behaviour and are of excellent agreement with reliable benchmark solutions. In addition, the preliminary parametric study has shown that the stress intensity factor along the crack front is significantly reduced as the thickness of the patch increases while the reverse trend has been observed for the adhesive layer.

Acknowledgements

The authors gratefully acknowledge the supports provided by the JICA Project for AUN/SEED-Net and The Thailand Research Fund (Grant No. RSA5980032).

References

- [1] Arendt C and Sun CT. Bending effects of unsymmetric adhesively bonded composite repairs on cracked aluminum panels, 1994.
- [2] Sun CT, Klug J, Arendt C. Analysis of cracked aluminum plates repaired with bonded composite panels. AIAA Journal, 34(2), pp. 369-74, 1996.

- [3] Baker AA, Jones R. Bonded repair of aircraft structures. Dordrecht: Martinus Nijhoff, 1988.
- [4] Rose LRF. An application of the inclusion analogy for bonded reinforcements. *International Journal of Solids and Structures*, 17(8), pp. 827-838, 1981.
- [5] Jones R. Bonded repair of damage. *Journal of the Aeronautical Society of India*, 1984.
- [6] Young A, Rooke DP, Cartwright DJ. Analysis of patched and stiffened cracked panels using the boundary element method. *International journal of solids and structures*, 29(17), pp. 2201-2216, 1992.
- [7] Liu HB, Zhao XL, Al-Mahaidi R. Boundary element analysis of CFRP reinforced steel plates. *Composite Structures*, 91(1), pp. 74-83, 2009.
- [8] Pisa CD, Aliabadi MH. Boundary element analysis of stiffened panels with repair patches. *Engineering Analysis with Boundary Elements*, 56, pp. 162-175, 2015.
- [9] Salgado NK, Aliabadi MH. The application of the dual boundary element method to the analysis of cracked stiffened panels. *Engineering Fracture Mechanics*, 54(1), pp. 91-105, 1996.
- [10] Salgado NK, Aliabadi MH. The boundary element analysis of cracked stiffened sheets, reinforced by adhesively bonded patches. *International journal for numerical methods in engineering*, 42(2), pp. 195-217, 1998.
- [11] Sekine H, Yan B, Yasuho T. Numerical simulation study of fatigue crack growth behavior of cracked aluminum panels repaired with a FRP composite patch using combined BEM/FEM. *Engineering Fracture Mechanics*, 72(16), pp. 2549-2563, 2005.
- [12] Jiann-Quo T, Kam-Lun S. Analysis of cracked plates with a bonded patch. *Engineering Fracture Mechanics*, 40(6), pp. 1055-1065, 1991.
- [13] Alaimo A, Milazzo A, Orlando C. Boundary elements analysis of adhesively bonded piezoelectric active repair. *Engineering fracture mechanics*, 76(4), pp. 500-511, 2009.
- [14] Useche J, Sollero P, Albuquerque EL, Palermo L. Boundary element analysis of cracked thick plates repaired with adhesively bonded composite patches. *SDHM: Structural Durability & Health Monitoring*, 4(2), pp. 107-116, 2008.
- [15] Wen PH, Aliabadi MH, Young A. Stiffened cracked plates analysis by dual boundary element method. *International journal of fracture*, 106(3), pp. 245-258, 2000.
- [16] Wen PH, Aliabadi MH, Young A. Boundary element analysis of flat cracked panels with adhesively bonded patches. *Engineering fracture mechanics*, 69(18), pp. 2129-2146, 2002.
- [17] Wen PH, Aliabadi MH, Young A. Boundary element analysis of curved cracked panels with adhesively bonded patches. *International journal for numerical methods in engineering*, 58(1), pp. 43-61, 2003.
- [18] Widagdo D, Aliabadi MH. Boundary element analysis of cracked panels repaired by mechanically fastened composite patches. *Engineering analysis with boundary elements*, 25(4-5), pp. 339-345, 2001.
- [19] Yu QQ, Zhao XL, Chen T, Gu XL, Xiao ZG. Crack propagation prediction of CFRP retrofitted steel plates with different degrees of damage using BEM. *Thin-Walled Structures*, 82, pp. 145-158, 2014
- [20] Rungamornrat J, Mear ME. Weakly-singular, weak-form integral equations for cracks in three-dimensional anisotropic media. *International Journal of Solids and Structures*, 45(5), 1283-1301, 2008a.
- [21] Hughes TJ. *The finite element method: linear static and dynamic finite element analysis*, Courier Corporation, 2012.
- [22] Bathe KJ. *Finite element procedures*, Klaus-Jurgen Bathe, 2006.
- [23] Zienkiewicz OC, Taylor RL. *The finite element method: solid mechanics*, Butterworth-heinemann, 2000.
- [24] Rungamornrat J, Mear ME. A weakly-singular SGBEM for analysis of cracks in 3D anisotropic media. *Computer Methods in Applied Mechanics and Engineering*, 197(49-50), pp.4319-4332, 2008b.
- [25] Li S, Mear ME, Xiao L. Symmetric weak-form integral equation method for three-dimensional fracture analysis. *Computer Methods in Applied Mechanics and Engineering*, 151(3-4), pp.435-459, 1998.
- [26] Yates JR, Zanganeh M, Tai YH. Quantifying crack tip displacement fields with DIC. *Engineering Fracture Mechanics*, 77, pp. 2063-2076, 2010.
- [27] Rungamornrat J, Sukulthanasorn N, Mear ME. Analysis for T-stress of cracks in 3D anisotropic elastic media by weakly singular integral equation method. *Computer Methods in Applied Mechanics and Engineering*, 347, pp. 1004-1029, 2019.
- [28] Xiao L. Symmetric weak-form integral equation method for three-dimensional fracture analysis. Ph.D. Dissertation, University of Texas at Austin, USA, 1998.